Model-driven directed-energy-deposition process workflow incorporating powder flowrate as key parameter

Kellen D. Traxel, Darin Malihi, Kyler Starkey and Amit Bandyopadhyay W. M. Keck Biomedical Materials Research Laboratory School of Mechanical and Materials Engineering Washington State University, Pullman, WA 99164, USA E-mail: amitband@wsu.edu

Highlights

- A successful process-comparison parameter was formulated for directed energy deposition of Ti6Al4V.
- Increased laser power and scan speed results in higher track width at limited expense of unmelted powder.
- Varying combinations of laser power, scan speed, and powder flowrate at constant comparison parameter result in quality tracks with >99% relative density when processed into bulk structures using industrial equipment.

Abstract

Process optimization for directed-energy-deposition, an industrial laser-based additive manufacturing technique, is a time-intensive endeavor for manufacturers. Herein we investigate the use of a modified analytical process-model based on powder-bed-fusion techniques, to predict quality build parameters by incorporating the effects of three key parameters: laser-power, scanning-speed, and powder flowrate. Titanium alloy (Ti6Al4V) tracks of varying parameters were built, studied, and used to predict parameters for quality builds used at different parameters. The model agreed well with experimental build quality at powder flowrates less than 6.5g/min, whereas, higher flowrates created significant unmelted-particle regions, despite optimal parameter predictions. Processing of multi-layer bulk samples revealed that parameters in the optimal range account for relative densities >99%, indicating quality bulk processing parameters. Our results indicate that process modeling with the incorporation of powder feedrate as a key parameter is possible using a commercial laser-based additive manufacturing system.

Keywords: additive manufacturing, process modeling, Ti6Al4V, directed energy deposition

1. Introduction

Metal additive manufacturing (AM) has rapidly changed the engineering landscape owing to the new designs and fabrication strategies possible in comparison to traditional manufacturing methods [1]. One powder-based laser metal-AM method, directed energy deposition (DED), has been exploited for its ability to easily repair existing structures [2], change feedstock composition during processing [3], and combine hybrid additive and subtractive processes. While promising, challenges exist optimizing many processing parameters. Current advances in this area involve machine learning or thermomechanical modeling-based techniques to predict optimal parameter ranges, but lack experimental data that are specific to each AMmethod [4–7]. Machine vision and machine learning based approaches have been successful in predicting optimal parameters in the case of powder-bed-fusion (PBF) [8,9], a laser-based metal-

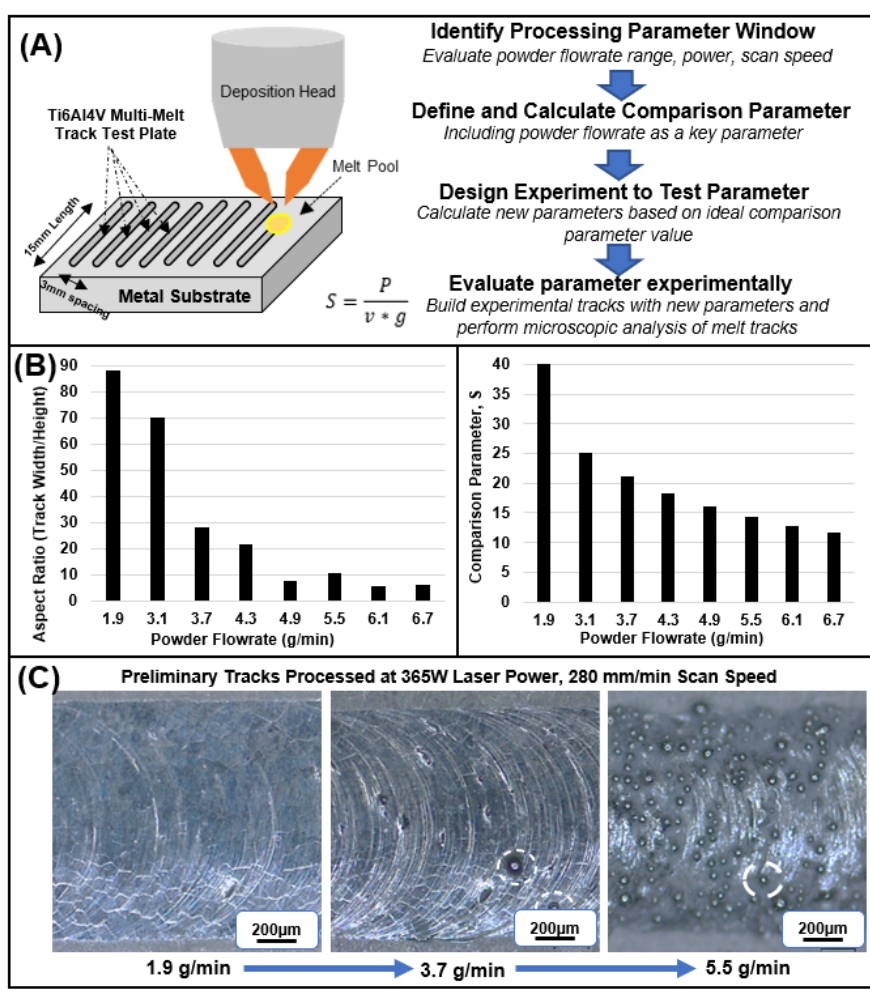


Figure 1: Processing schematic and initial print characteristics by varying powder flowrate. **(A)** LENSTM schematic **(B)** Initial deposition tracks with variable powder flowrate **(C)** Characteristics of builds of variable flowrate.

AM technique well suited for small parts and fine features but with low layer thicknesses (20-60μm). This previous work, along with the foundational work of Simchi (2003) has led to a key-relationship between the processing parameters - laser power, scanning speed, layer thickness, and hatch spacing, but doesn't translate explicitly for **DED-based** processing [10],

where building /

repairing a large structure is critical, and the 200-500µm layer thicknesses in DED are ideal. Among other aspects, the key difference between the PBF and DED method is the presence of powder flow into the focal point of the laser, resulting in variable layer thicknesses and build quality if parameters are not well tuned. Because of this, an experimentally-driven unifying comparison parameter for DED would be useful to inform the aforementioned modeling approaches. The current work involves the creation of a comparison parameter between laser power, scan speed, and powder flowrate (Eq. 1), defined in a similar manner to the PBF relationship [10]. Using this proposed relationship, an optimal comparison parameter value was experimentally determined using single-track arrays, and a second experiment designed to evaluate the efficacy of the model when deviating from the quality comparison parameter value. Bulk structures were subsequently built in high-throughput build ranges and density analysis was performed to demonstrate the ability to use the model in the prediction of quality parameters for bulk structures.

2. Materials and methods

Experimental single-tracks (see **Fig. 1A and Table 1**) were deposited using Ti-6Al-4V Gr.5 powder (Tekna, Quebec, CA) via OPTOMEC LENSTM powder-fed additive manufacturing system (MR700, Albuquerque, NM), operating a 500W Nd-YAG laser, inert-gas feed system and environmentally-controlled chamber (O₂<10ppm), more information can be found in ref. [11]. To identify the LENSTM system processing range, preliminary tracks and parameter sets

Table 1: Processing parameters used for experimental single-track study.

Strategy	Track ID	Laser Power (W)	Scanning Speed (mm/min)	Powder Flowrate (g/min)
Adjust: Laser Power Maintain: Powder Flowrate Calculate: Scanning Speed	1	275	217	3.1
	2	347	273	
	3	418	330	
Adjust: Scanning Speed Maintain: Laser Power Calculate: Powder Flowrate	4	365	241	7.3
	5		280	4.3
	6		305	2.74
Adjust: Powder Flowrate Maintain: Laser Power Calculate: Scanning Speed	7	365	299	1.9
	8		277	4.3
	9		258	6.7

were centered around initial parameters shown to be successful in previous works [11], with only the powder flowrate altered, and the resulting track aspect ratio and comparison parameter used in this study plotted in **Fig. 1B**. The proposed comparison parameter, *S*, found insightful from the preliminary data is defined as:

$$S = \frac{P}{v * g} \quad (1)$$

Where P is the laser power (W), v is the scan speed (mm/min) and g is the powder feed rate (g/min), for final units of W*min² g⁻¹mm⁻¹. The comparison parameter is analogous to Simchi's energy input relationship, where increased power and decreased scanning speed results in higher overall energy input to the material. With the addition of powder flowrate the overall energy input decreases due to the increase in mass delivered to the melt pool and energy required

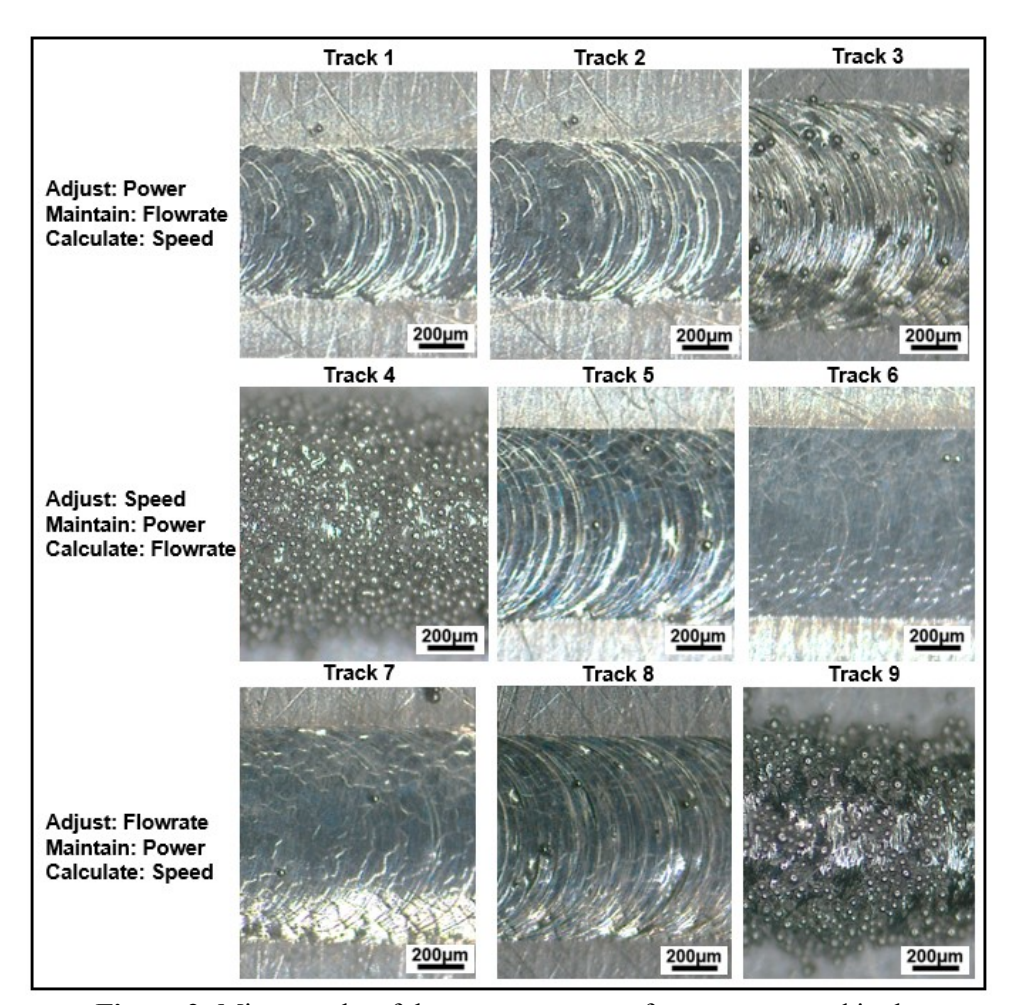


Figure 2: Micrographs of three separate sets of parameters used in the development experiment (S-parameter ranging from 14-18 W*min² g⁻¹mm⁻¹).

to melt the subsequent material [10]. Adequate melting of particles was the main determining factor for a quality build, where other factors such as aspect ratio and build height were secondary indications of a parameter set's efficacy. From the preliminary builds, the S-

value for the optimal build (14-18 W*min² g⁻¹mm⁻¹) was used to design another set of parameters for a second set of tracks to determine the model's validity. Three separate approaches with each set of three tracks having one variable held constant, one varied, and the final calculated using the proposed relationship at optimal S-value ranges. It is important to note that while the relationship incorporates powder flowrate, the LENS™ system's powder flowrate control is an impeller input voltage, so the voltage value was used in the determination of quality parameters, with flowrates calculated externally via collection container and then reported here. All parameters were bounded by the confines of the machine (500W and externally-calculated max powder flowrate of 7.3 g/min). Additional bulk structures were processed in a high throughput range (1000-1300mm/min) within a FormAlloy (San Diego, CA, USA) industrial DED system utilizing a 500W-fiber laser and coaxial feed system, with powder flowrate and laser powers chosen that replicate similar high-quality LENS™ tracks, with relative densities evaluated using Archimedes method (see Fig. 3).

3. Results and Discussion

All single tracks (Fig. 1) resulted in heights of 20-250 µm and widths of 1.8-1.4 mm. The injection of higher amounts of powder resulted in higher buildup, decreasing track aspect ratio, and unmelted particles on the track surfaces (Fig. 1C). At lower powder flowrates and higher overall energy input (1.9g/min & 3.7 g/min), the circular weld outline can readily be observed, whereas at higher flowrates (lower energy input) this outline was not as apparent. From all preliminary tracks, it was decided that a flowrate of 4.9g/min provided both sufficient melt while also delivering track height of 178µm, which is common for DED-processed materials (comparison parameter equal to 16). From the calculated parameters, Tracks 1 & 2 had similar characteristics, i.e., limited unmelted particle regions and readily visible circular weld lines, indicative of quality build parameters and input energy efficiency. Track 3, however, maintained the same melt-track visibility while also being wider in diameter in comparison to the other tracks, owing to the increased power provided even at higher scanning speed, indicating that the build optimization strategy of increased power and scan speed at constant flowrate tends to create tracks with increased width and height at limited expense of unmelted power. Further, track 4 shows that higher powder flowrate results in a track that, despite being predicted as adequate parameters via the model, maintains unmelted particles on the track surface. This

specific parameter combination included the highest amount of powder flowrate attempted (7.3g/min). For tracks 5 & 6, higher scan speed (280 -305mm/min) and corresponding lower powder flowrate (ascalculated) results in tracks that are completely melted and have

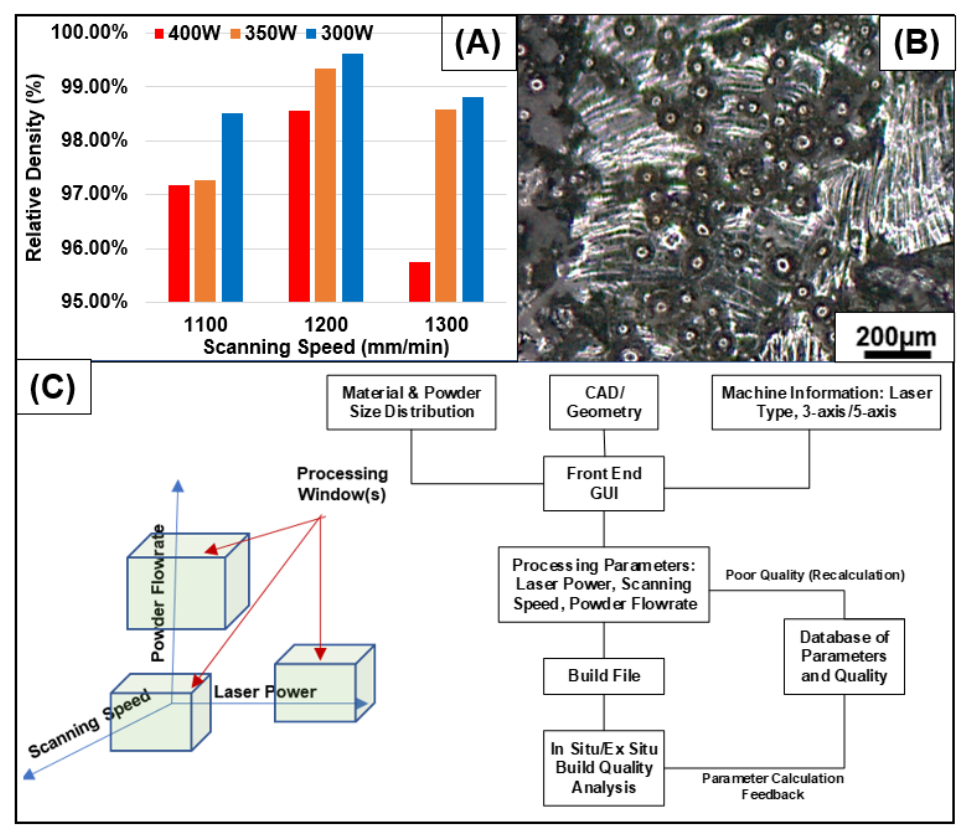


Figure 3: Translating single layer model into a multi-layer components. (A) Measured densities of bulk samples built in regions defined by optimal parameters. (B) Top surface optical micrograph of the 300W, 1200mm/s processing parameters. (C) Proposed workflow for using the present model when developing parameter sets for directed energy deposition.

visible weld-track lines, indicative of quality builds. This set of tracks confirmed that higher flowrate at limited change in laser power or scanning speed results in poorer track quality. Tracks 7 & 8 resulted in sufficient melt with weld tracks visibly clear at powder flowrates of 1.9g/min and 4.3g/min respectively, indicating quality build parameters. Track 9, however, at a powder flowrate of 6.7g/min maintained high regions of unmelted particles and surface roughness, indicative of a poor-quality build with low energy efficiency put into the track. Bulk samples were processed in the FormAlloy system at varying parameters (**Fig. 3A**) resulting in similar track qualities to tracks 5 & 6 (**Fig. 3B**). The bulk samples exhibited relative densities ranging from 95.0%-99.5%, indicating that quality builds assessed in the track-scale can be applied towards larger scale components.

From **Fig. 2**, the proposed model predicts adequate processing parameters for all combinations of laser power and scanning speed, with powder flowrate in the range from 1.9-

4.3g/min. As shown in experimental tracks 1-3, 5-6, 7-8 (powder flowrates below 6.7g/min), the tracks exhibit sufficient melting and readily-visible weld-track lines. It is clear from tracks 4 and 5, that powder flowrates above 6.7g/min result in significant amounts of unmelted particles and limited visibility of weld-track lines, where powder feed rate becomes too high and most of the particles are no longer able to melt completely. Similar overall features have been observed in PBF-tracks where lower energy results in unmelted regions, and the converse resulted in more visible track features [12]. In comparison to PBF, DED machines can adjust parameters in situ, indicating that PBF tracks that have a poor combination of high laser power/low scan speed will result in melt-pool keyholes [13], which (in DED) can be alleviated via powder flowrate adjustment (as is shown from tracks 1-3 in Fig. 2). To this end, it is envisioned that a feedback loop workflow similar to that shown in Fig. 3C could be realized with inputs such as the material, geometry and machine information, fed into a GUI where the use of the developed governing equations calculate the optimal processing parameters. A build file is then generated and then ex situ/in situ quality analysis is performed to determine the efficacy of the parameters for generating a quality build, adding to an existing database to improve future builds with varying geometry and material/machine information.

4. Conclusions

Processing-parameter modeling was investigated for laser-based additive manufacturing using directed energy deposition method. The model sufficiently predicted quality build parameters for all combinations of laser power and scanning speed, with powder flowrates in the range of 1.9-4.3g/min, while higher powder flowrates tended to dominate the melt pool and result in significant unmelted particle regions. Our parameters (translating to >99% relative density parts) indicate that an analytical approach can be used to determine processing parameters for next generation additive manufacturing equipment.

5. Acknowledgements

Authors would like to acknowledge financial support from the National Science Foundation under the grant number NSF-CMMI 1538851 (PI - Bandyopadhyay) and NSF-CMMI 1934230 (PI - Bandyopadhyay).

6. Declaration of Interest: None

7. References

- [1] Tofail SAM, Koumoulos EP, Bandyopadhyay A, Bose S, O'Donoghue L, Charitidis C. Additive manufacturing: scientific and technological challenges, market uptake and opportunities. Mater Today 2018;21:22–37. https://doi.org/10.1016/j.mattod.2017.07.001.
- [2] Shamsaei N, Yadollahi A, Bian L, Thompson SM. An overview of Direct Laser Deposition for additive manufacturing; Part II: Mechanical behavior, process parameter optimization and control. Addit Manuf 2015. https://doi.org/10.1016/j.addma.2015.07.002.
- [3] Bandyopadhyay A, Heer B. Additive manufacturing of multi-material structures. Mater Sci Eng R Reports 2018;129:1–16. https://doi.org/10.1016/j.mser.2018.04.001.
- [4] Bandyopadhyay A, Traxel KD. Invited review article: Metal-additive manufacturing—Modeling strategies for application-optimized designs. Addit Manuf 2018;22:758–74. https://doi.org/10.1016/j.addma.2018.06.024.
- [5] Qi X, Chen G, Li Y, Cheng X, Li C. Applying Neural-Network-Based Machine Learning to Additive Manufacturing: Current Applications, Challenges, and Future Perspectives. Engineering 2019;5:721–9. https://doi.org/10.1016/j.eng.2019.04.012.
- [6] Frazier WE. Metal additive manufacturing: a review. J Mater Eng Perform 2014;23:1917–28. https://doi.org/10.1007/s11665-014-0958-z.
- [7] Gobert C, Reutzel EW, Petrich J, Nassar AR, Phoha S. Application of supervised machine learning for defect detection during metallic powder bed fusion additive manufacturing using high resolution imaging. Addit Manuf 2018;21:517–28. https://doi.org/10.1016/j.addma.2018.04.005.
- [8] Aoyagi K, Wang H, Sudo H, Chiba A. Simple method to construct process maps for additive manufacturing using a support vector machine. Addit Manuf 2019;27:353–62. https://doi.org/10.1016/j.addma.2019.03.013.
- [9] Scime L, Beuth J. Using machine learning to identify in-situ melt pool signatures indicative of flaw formation in a laser powder bed fusion additive manufacturing process. Addit Manuf 2019;25:151–65. https://doi.org/10.1016/j.addma.2018.11.010.
- [10] Simchi A, Pohl H. Effects of laser sintering processing parameters on the microstructure and densification of iron powder. Mater Sci Eng A 2003. https://doi.org/10.1016/S0921-5093(03)00341-1.
- [11] Traxel KD, Bandyopadhyay A. Reactive-deposition-based additive manufacturing of Ti-Zr-BN composites. Addit Manuf 2018;24. https://doi.org/10.1016/j.addma.2018.10.005.
- [12] Caggiano A, Zhang J, Alfieri V, Caiazzo F, Gao R, Teti R. Machine learning-based image processing for on-line defect recognition in additive manufacturing. CIRP Ann 2019;68:451–4. https://doi.org/10.1016/j.cirp.2019.03.021.
- [13] Teng C, Pal D, Gong H, Zeng K, Briggs K, Patil N, et al. A review of defect modeling in laser material processing. Addit Manuf 2017;14:137–47. https://doi.org/10.1016/j.addma.2016.10.009.